Extremophiles (2012) 16:115–125
DOI 10.1007/s00792-011-0411-2

ORIGINAL PAPER

Complementation of *Sulfolobus solfataricus* PBL2025 with an α-mannosidase: effects on surface attachment and biofilm formation

A. Koerdt · S. Jachlewski · A. Ghosh · J. Wingender · B. Siebers · S.-V. Albers

Received: 29 July 2011 / Accepted: 2 November 2011 / Published online: 18 November 2011

Abstract Compared to *Sulfolobus solfataricus* P2, the *S. solfataricus* mutant PBL2025 misses 50 genes (SSO3004-3050), including genes coding for a multitude of enzymes possibly involved in sugar degradation or metabolism. We complemented PBL2025 with two of the missing proteins, the α-mannosidase (SSO3006, Ssα-man) and the β-galactosidase LacS (SSO3019), and performed comparative fluorescence microscopy and confocal laser scanning microscopy to analyze the recombinant strains. We demonstrated that the Ssα-man complemented strain resembled the *S. solfataricus* P2 behavior with respect to attachment of cells to glass and growth of cells in static biofilms. During expression of the Ssα-man, but not LacS, glucose and mannose-containing extracellular polymeric substance (EPS) levels changed in the recombinant strain during surface attachment and biofilm formation. These results suggest that the Ssα-man might be involved in the modulation of the EPS composition and/or in the de-mannosylation of the glycan tree, which is attached to extracellular glycosylated proteins in *S. solfataricus*. On the other hand, LacS expression in PBL2025 reduced the carbohydrate content of the isolated total EPS implying a role in the modulation of the produced EPS during static biofilm formation. These are the first enzymes identified as playing a role in archaeal EPS formation.

Keywords Archaea · Extracellular polymeric substances (EPS) · α-Mannosidase · Glycosylation · Surface attachment · Biofilm · Lectin staining

Communicated by A. Driessen.

A. Koerdt · A. Ghosh · S.-V. Albers (✉)
Molecular Biology of Archaea, Max Planck Institute for Terrestrial Microbiology, Karl-von-Frisch-Strasse, 35043 Marburg, Germany
e-mail: albers@mpi-marburg.mpg.de

S. Jachlewski · B. Siebers
Molecular Enzyme Technology and Biochemistry (MEB), Faculty of Chemistry, Biofilm Centre, University of Duisburg-Essen, Universitätsstr. 5, 45141 Essen, Germany

J. Wingender
Aquatic Microbiology, Biofilm Centre, Faculty of Chemistry, University of Duisburg-Essen, Universitätsstr. 5, 45141 Essen, Germany

Introduction

Biofilms are microbial populations that adhere to each other and/or to interfaces (usually solid–liquid) and are typically surrounded by a matrix of extracellular polymeric substances (EPS). Bacterial EPS mainly consist of polysaccharides, proteins, DNA and lipids; they determine the structural and functional integrity of bacterial biofilms, and contribute significantly to the organization of biofilm communities (Flemming and Wingender 2010). In contrast to bacterial biofilms, relatively little information exists on biofilms and EPS of archaea, although there are indications that they are also capable of biofilm formation (Baker-Austin et al. 2010; Koerdt et al. 2010; Rinker and Kelly 1996; Schopf et al. 2008), some archaea have been shown to produce and secrete extracellular polysaccharides (Albers and Meyer 2011). While *Thermococcus litoralis* only produces mannose-containing carbohydrates (Rinker and Kelly 1996, 2000), haloarchaea and Sulfolobales secrete sulfated exopolysaccharides containing the sugar residues glucose, galactose and rhamnose (Antón et al. 1988; Nicolaus et al. 1993; Paramonov et al. 1998).

Most of the extracellular proteins of archaea have been shown to be *N*- and/or *O*-glycosylated. *O*-linked glycans, which are linked via hydroxyl oxygens to Ser or Thr residues have been found in the S-layer proteins of *Halobacterium salinarum* and *Haloferax volcanii* (Mescher and Strominger 1976; Sumper et al. 1990). However, detailed studies have only been performed on the N-glycosylation pathway in archaea and demonstrate that the pathway includes aspects from both the eukaryal and bacterial pathways. Archaeal *N*-glycans, which are covalently linked to the nitrogen of Asn residues, show an impressive diversity of glycans ranging from linear glycans that encompass even amino acids in methanogens to tri-branched eukarya-like chitobiose-bearing glycans in Sulfolobales (Abu-Qarn et al. 2007; Kelly et al. 2009; Peyfoon et al. 2010; Voisin et al. 2005).

Recently, an α-mannosidase (SSO3006, Ssα-man) of *S. solfataricus*, belonging to the glycoside hydrolase family 38 (GH38), was shown to catalyze the degradation of α(1, 2), α(1, 3) and α(1, 6)-D-mannobiose in vitro, thus exhibiting a broad substrate specificity. In addition, the enzyme has been shown to de-mannosylate high-mannose oligosaccharides (e.g., Man3GlcNAc2, Man7GlcNAc2) commonly found in glycoproteins (Cobucci-Ponzano et al. 2010). Most importantly, also the de-mannosylation of *N*-glycosylated proteins (RnaseB) was demonstrated and, therefore, an involvement in protein glycosylation has been postulated (Cobucci-Ponzano et al. 2010). While in bacteria GH38 mannosidases are involved in diverse catabolic and metabolic reactions (Maruyama et al. 1994; Nakajima et al. 2003; Sampaio et al. 2004), in eukarya they have been proven to be involved in the trimming of the glycan tree in the endoplasmic reticulum (Herscovics 1999).

The thermoacidophilic crenarchaea *Sulfolobus* spp. contain a high number of *N*-glycosylated extracellular proteins such as substrate-binding proteins, the S-layer protein and flagellins (Albers et al. 1999). For *Sulfolobus acidocaldarius*, it was shown that the tri-branched glycan tree of the S-layer protein contains three mannose sugar residues (Peyfoon et al. 2010). Moreover, *Sulfolobus solfataricus* cells attached to a glass surface produced EPS that contained glucose, mannose, galactose and *N*-acetylglucosamine (Zolghadr et al. 2010). Similarly, other Sulfolobales strains secreted clouds of EPS during static biofilm formation (Koerdt et al. 2010).

Interestingly, it was observed that in contrast to *S. solfataricus* P2, PBL2025, a spontaneous mutant, which is derived from *S. solfataricus* 98/2 (Schelert et al. 2004), formed microcolonies, which secreted a higher amount of EPS (Zolghadr et al. 2010). Among the 50 genes that are absent in PBL2025 compared to *S. solfataricus* P2 are many sugar degrading, modulating and transporting proteins (Schelert et al. 2004), including the Ssα-man. RT-PCR studies revealed that the Ssα-man was significantly induced in glass-attached cells compared to planktonic cells (Zolghadr et al. 2010) leading to the hypothesis that the Ssα-man might also be involved in the modulation of EPS (Zolghadr et al. 2010). LacS (SSO3019), a well described β-glycosidase of *S. solfataricus* P2 (Cubellis et al. 1990; Moracci et al. 2001), is also one of the sugar degrading enzymes that are missing in PBL2025. This enzyme has a broad spectrum of activity toward substrates including β-galactosides and their chemical analogs. Therefore, addition of X-Gal leads to a blue coloration of LacS-containing cells and it has been demonstrated that LacS is essential for growth of *S. solfataricus* P2 in lactose minimal media (Bartolucci et al. 2003). Like the Ssα-man, LacS was upregulated during attachment of *S. solfataricus* cells to glass surfaces (Zolghadr et al. 2010).

In this study, we have expressed the Ssα-man and LacS from *S. solfataricus* P2 in PBL2025 and compared the recombinant strains to *S. solfataricus* P2 regarding their behavior during surface attachment, biofilm and EPS formation. Comparative confocal laser scanning microscopy (CLSM) and the isolation and quantitative analysis of EPS of these strains demonstrated the possible function of the Ssα-man in the modulation of the EPS or the intracellular de-mannosylation of the glycan tree prior to transfer to the extracellular glycoproteins.

Materials and methods

Strains and media

Sulfolobus solfataricus P2, PBL2025 (Schelert et al. 2004), PBL2025-ABCE1, PBL2025-LacS (Albers et al. 2006) and PBL2025-Ssα-man were aerobically grown in liquid Brock medium (Brock et al. 1972) with a pH of 3 at 76°C. The medium was supplemented either with 0.1% (w/v) tryptone or with 0.1% (w/v) N-Z-amine, 0.2% (w/v) glucose and 0.2% (w/v) D-arabinose for expression purposes. The growth of the cells was monitored by measurement of the optical density at 600 nm.

Cloning of Ssα-man, LacS and ABCE1 in virus-based vector for expression in PBL2025

The α-mannosidase gene (*SSO3006*) was amplified from the genomic DNA of *S. solfataricus* P2. The restriction sites *Bam*HI and *Nco*I were incorporated into the PCR product using the primers 5′-TTCCCATGGGAAGAAACATAAACGAGC-3′ and 5′-TTCGGATCCACCCCTCACACTTATTG-3′, respectively. Cloning of the *Nco*I/*Bam*HI digested PCR product into pMZ1 resulted in plasmid pSVA620 (Zolghadr et al. 2007), expressing SSO3006 with

a C-terminal tandem tag (Strep-10× His-tag) under the control of the p*ara*S (Albers et al. 2006). The expression construct pSVA621 was generated by digesting pSVA620 with *Eag*I/*Bln*I, followed by ligation of the digested insert to pre-digested pSVA9, thereby replacing *lacS* in the multiple cloning site of pSVA9. For homologous expression of the β-galactosidase LacS (SSO3019) (Bartolucci et al. 2003) in PBL2025, we used the virus-based vector pSVA9, which contains the β-galactosidase *lac*S under control of the arabinose-inducible promoter *paraS* (Albers et al. 2006). The control expression plasmid pSVA31 contained ABCE1 (SSO0287), a cytoplasmic protein involved in ribosome recycling (Barthelme et al. 2011), under the control of the p*ara*S promoter with a C-terminal tandem tag (Albers et al. 2006). The constructs pSVA621, pSVA9 and pSVA31 were electroporated into PBL2025, which was grown in medium containing 0.1% N-Z-amine, 0.2% glucose and 0.2% D-arabinose as previously described (Zolghadr et al. 2007). The expression of either α-mannosidase (pSVA621) or ABCE1 (pSVA31) was verified by SDS-PAGE followed by Western blotting. Expression of LacS was tested by a colorimetric assay as described in Albers et al. (2006). All constructed plasmids were verified by sequencing.

Attachment assay, fluorescence and differential interference contrast microscopy

Microscopy was performed as described in Zolghadr et al. (2010). Briefly, the cells were grown for 24 h in 40 mL medium containing 0.1% N-Z-amine, 0.2% glucose and 0.2% D-arabinose in the presence of an objective glass slide in 100 mL Schott flasks as shaking cultures at 76°C (RPM, Abmessung Glas). The inoculation OD_{600} was 0.01. After 24 h, the glass slides were removed from the Schott flasks, washed with Brock medium and then incubated in 5% formaldehyde containing Brock medium with a pH of 5. Light microscopy was performed with fixed cells on the glass slides. For lectin staining, the glass slides were incubated with 15 μl of concanvalin A (ConA, 5 mg/mL, Invitrogen, Karlsruhe, Germany). After lectin staining, glass slides were incubated in the dark for 20 min. Prior to microscopy analysis, the glass slides were washed once more with Brock medium (pH 5).

Biofilm growth and confocal laser scanning microscopy

CLSM was performed as described in Koerdt et al. (2010). Briefly, the cells were inoculated to grow static biofilms with an OD_{600} of 0.03 in hydrophobic microscopy plastic dishes (μ-dishes, 35-mm high; Ibidi, Martinsried). The biofilms were either cultivated in 3 mL of Brock medium supplemented with 0.1% tryptone or medium containing 0.1% N-Z-amine, 0.2% glucose and 0.2% D-arabinose for expression under static conditions at 75°C for 3 days, with an exchange of the media (see above) after every 24 h. The biofilm was stained with 6 μl DAPI (4′,6-diamidino-2-phenylindole, 300 μg/mL), 15 μl fluorescein-conjugated ConA (5 mg/mL; Invitrogen, Karlsruhe, Germany), specific for α-mannopyranosyl and α-glucopyranosyl residues and 8 μl Alexa Fluor® 594 conjugated isolectin GS-IB_4 (IB_4) (*Griffonia simplicifolia* 1 mg/mL; Invitrogen, Karlsruhe, Germany), binding to α-D-galactosyl residues. The staining solutions were incubated for at least 20 min at room temperature. Before the CLSM images were taken with an inverted TCS-SP5 confocal microscope (Leica, Bensheim, Germany), unbound lectins were removed by washing of the biofilm with Brock medium (pH 5). The obtained data were analyzed using the program IMARIS (Bitplane AG, Zürich, Switzerland).

Overexpression of Ssα-man (SSO3006), LacS (SSO3019) and ABCE1 (SSO0287) in PBL2025

Twenty milliliters of an overnight culture of PBL2025 cells harboring either the pSVA9, pSVA31 or pSVA621 overexpression plasmids were used to inoculate 300 mL of Brock medium containing 0.1% *NZ*-amine and 0.2% D-arabinose. Cells were grown at 76°C until an OD_{600nm} of 0.8 was reached. The cells were collected by centrifugation, resuspended in lysis buffer [50 mM HEPES–NaOH, pH 7.5, 150 mM NaCl, 10% (v/v) glycerol] containing the complete EDTA-free protease inhibitor cocktail (1 tablet/50 mL of lysate; Roche, Manheim, Germany), frozen in liquid nitrogen and stored at −80°C.

Purification of recombinant proteins

Prior to purification, frozen resuspended cell pellets were thawed on ice. Cells were lysed by sonication with a Sonoplus HD3100 sonicator (Bandelin Sonorex Biotechnique, Germany) using probe HD3100 (60%, 1 min on, 1 min off for 20 min). Cell debris was removed by centrifugation at 6,000×*g* for 15 min followed by centrifugation at 150,000×*g* for 30 min at 4°C in an Optima™ MAX-XP ultracentrifuge (rotor MLA 55) (Beckman Coulter, USA) to remove membranes. The supernatant was used for histidine affinity chromatography using the Profinia™ protein purification system (BioRad Laboratories, Inc, USA) following the manufacturer's protocol. Briefly, for the purification of His-tagged proteins, the supernatant was applied to an Ni^{2+}-affinity column (Native IMAC) on the Profinia™ protein purification system. The bound protein was eluted in lysis buffer containing 500 mM of imidazole. Protein purity was monitored by sodium dodecyl sulfate–polyacrylamide gel electrophoresis (SDS-PAGE). Gels were stained with Biosafe (BioRad Laboratories, Inc, USA) protein stain.

Protein concentration was determined with the BioRad protein assay dye-dependent reagent (BioRad Laboratories, Inc, USA). To further check the expression and purification, Western blot analysis was performed using both anti-His (Sigma) and anti-Strep antibodies (BioRad Laboratories, Inc, USA).

EPS extraction and characterization

For EPS extraction, *S. solfataricus* P2, PBL2025, PBL2025-Ssα-man, PBL2025-LacS and PBL2025-ABCE1 were grown aerobically in shaking cultures in Brock medium supplemented either with 0.1% tryptone and 0.2% (w/v) glucose or with 0.1% (w/v) N-Z-amine, 0.2% (w/v) glucose and 0.2% (w/v) D-arabinose at 76°C. After 2 days of incubation, cultures were streaked on gellan gum-solidified Brock medium (6 g/L gellan gum; Gelzan™ CM Sigma-Aldrich, Munich, Germany) using an inoculation loop. The plates were sealed in plastic bags and incubated at 76°C for 4 days. The biomass was carefully scraped from the surface of the solid medium using a spatula, weighed and suspended in 6 mM of phosphate buffer (pH 7; 0.1 g of wet biomass per 10 mL). Total cell number was determined by DAPI staining (5 μg/mL, 20 min) and enumeration using an epifluorescence microscope at 1,000-fold magnification.

The biofilm suspensions were transferred into 50 mL centrifuge tubes in 10 mL aliquots. To each tube, 2 g of a hydrated cation exchange resin (Dowex® Marathon® C sodium from Sigma-Aldrich, Munich, Germany), which had been washed twice with phosphate buffer (pH 7, 15 min; 10 mL/g Dowex), was added. The samples were shaken at highest capacity for 20 min on a shaker (VortexGenie®2, Scientific Industries, New York, USA). Afterward, samples were centrifuged (20 min; 20,000×*g*; 4°C) and the supernatants (EPS and low molecular weight substances) were filter-sterilized (pore size 0.22 μm) (Rotilabo®, Roth, Karlsruhe, Germany) and dialyzed against deionized water using a dialysis membrane of 12–14 kDa MWCO. The dialyzed supernatant corresponded to the cell-free EPS solution. All extractions were performed in triplicate.

Protein and carbohydrate concentrations were determined using photometric methods. Carbohydrate concentrations were measured with the phenol sulfuric acid method (Dubois et al. 1956) using D-glucose as standard. For determination of protein concentrations, a modified Lowry assay was applied using bovine serum albumin as standard (Petersen 1977).

Results

Recently, it was demonstrated that surface-attached cells of a natural mutant of *S. solfataricus* 98/2, PBL2025, lacking 50 genes mainly involved in sugar metabolism and transport (Schelert et al. 2004), showed a highly increased production of EPS and a different structural appearance than *S. solfataricus* P2 (Zolghadr et al. 2010). To determine whether this difference was also apparent during biofilm formation, P2 and PBL2025 biofilms were grown for 3 days under aerobic static biofilm conditions in small Petri dishes at 76°C in Brock medium supplemented with 0.1% tryptone as described in Koerdt et al. (2010). To ensure optimal growth, the medium was exchanged every 24 h. The biofilms growing on the bottom of the Petri dishes were washed and stained with DAPI as well as fluorescently labeled lectins (ConA and IB_4). While DAPI binds to DNA, ConA binds to mannose and glucose residues and IB_4 to galactosyl residues. Previously, it was shown that extracellular proteins of *Sulfolobus* are *N*-glycosylated and contain sugars like glucose, galactose, mannose and *N*-acetylglucosamine (Albers et al. 1999). Moreover, the glycan structure of the *S. acidocaldarius* cytochrome $b_{558/566}$ and S-layer protein has been determined and contained mannose, *N*-acteylglucosamine, glucose and the sugar sulfoquinovose (Peyfoon et al. 2010; Zahringer et al. 2000). Additionally, biofilms of *S. tokodaii*, *S. acidocaldarius* and *S. solfataricus* were shown to produce EPS which reacted with ConA, IB4 and GSII (a *N*-acetylglucosamine specific lectin) (Koerdt et al. 2010). Therefore, ConA and IB_4 were chosen to analyze the established biofilms. The biofilms formed by *S. solfataricus* P2 and PBL2025 were similar with respect to cell density and thickness of the biofilms as observed by the DAPI signal (Fig. 1). Moreover, secretion of galactosyl containing EPS was comparable as demonstrated by staining with IB_4 lectin (Data not shown). However, a clear difference was observed in the ConA signal (Fig. 1). In PBL2025, a confluent staining with ConA was observed while *S. solfataricus* P2 exhibited an uneven, very low ConA signal indicating a lower production of glucose- and/or mannose-containing EPS or glycosylated cell surface proteins.

Expression of Ssα-man, LacS and ABCE1 in PBL2025

The lack of 50 genes in the genome of PBL2025 compared to *S. solfataricus* P2 and the previously shown induction of 8 of 18 tested genes of these 50 genes upon surface attachment suggested a possible function of these enzymes in production and modulation of the EPS (Zolghadr et al. 2010). Interestingly, the previously characterized enzymes α-mannosidase (Cobucci-Ponzano et al. 2010) and LacS (Cubellis et al. 1990) were among the induced genes.

A recent study by Cobucci-Ponzano et al. (2010) demonstrated that the recombinant α-mannosidase from *S. solfataricus* de-mannosylated oligosaccharides, which were frequently found in glycosylated proteins, and a

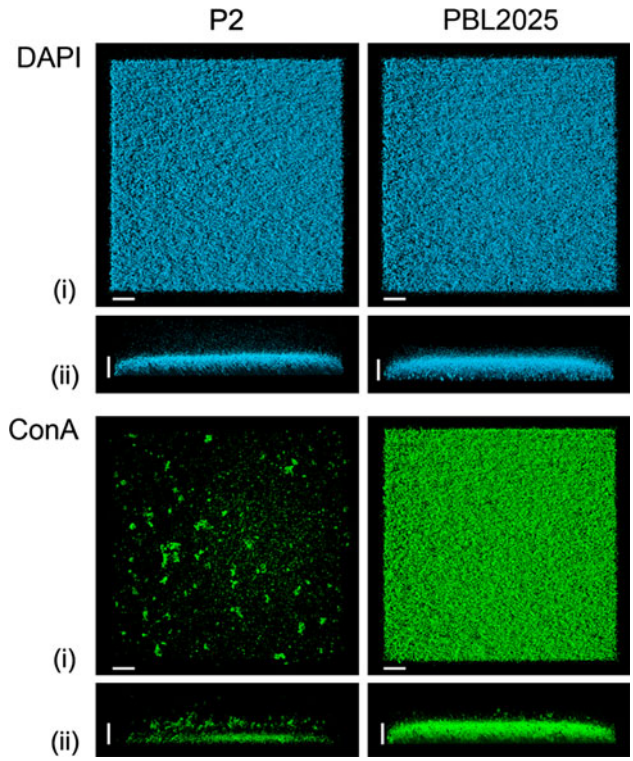

Fig. 1 CLSM analysis of 3-day-old *S. solfataricus* P2 and PBL2025 biofilm in petri dishes. The 3-day-old biofilms of *S. solfataricus* P2 (*left*, depicted as P2) and PBL2025 (*right*) were stained with DAPI (*blue signal*) and ConA (*green signal*) and analyzed by CLSM. *Bars* are 20 μm in length. *i* represents the top view and *ii* the side view of the biofilms, respectively

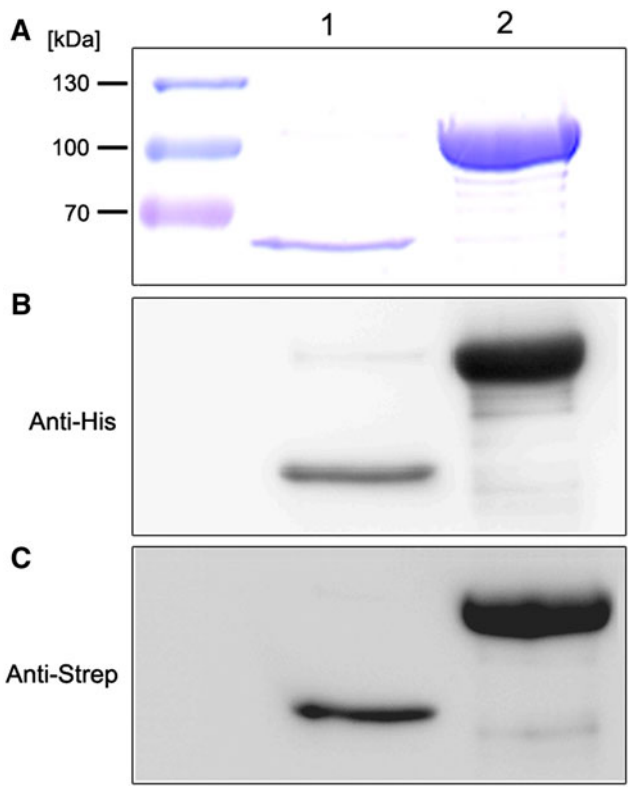

Fig. 2 Expression and His-tag purification of PBL2025-Ssα-man and PBL2025-ABCE1. **a** Coomassie blue-stained SDS-PAGE gel of the Ni affinity chromatography of cytoplasm, Western blot with **b** anti-His antibody and **c** anti-strep antibody of PBL2025-ABCE1 (Abu-Qarn et al. 2007) and PBL2025-Ssα-man (Albers et al. 1999)

possible role in the N-glycosylation pathway was suggested (Cobucci-Ponzano et al. 2010). Therefore, we used the available homologous *Sulfolobus* virus-based expression system (Albers et al. 2006; Jonuscheit et al. 2003) to complement PBL2025 with the α-mannosidase and *lacS* of *S. solfataricus* P2 to unravel their role in surface attachment, biofilm and EPS formation.

Five different strains, *S. solfataricus* P2, PBL2025 and PBL2025 complemented with either pSVA621 (PBL2025-Ssα-man), pSVA9 (PBL2025-LacS) or pSVA31 (PBL2025-ABCE1), were analyzed. ABCE1, a cytosolic protein involved in ribosome recycling was used as control in all experiments (Barthelme et al. 2007, 2011). To confirm that transformation of the plasmids into PBL2025 and expression of the proteins were successful, the recombinant ABCE1 and Ssα-man with C-terminal His- and Strep tag were purified via Ni^{2+} affinity chromatography. Analysis via SDS-PAGE of elution fractions revealed two dominant proteins of the expected molecular mass of 68 kDa for ABCE1 and 110 kDa for Ssα-man (Fig. 2a). To further confirm the identity of both proteins, immunoblotting with anti-His and anti-Strep antibodies was performed (Fig. 2c). Recombinant LacS was expressed without any affinity tag. Therefore, its expression was tested via a colorimetric assay, in which the colorless X-GAL was hydrolyzed by LacS resulting in blue coloration of the cells (data not shown).

Attachment of P2, PBL2025 and recombinant strains to glass

To determine whether alterations of EPS production of PBL2025 could be observed when Ssα-man or LacS were overexpressed in this strain, we analyzed the surface attachment from shaking culture in comparison to P2 and PBL2025-ABCE1 after 24 h. *S. solfataricus* P2 (Fig. 3, first row) and PBL2025 (Fig. 3, second row) showed a phenotype as described before (Zolghadr et al. 2010): *S. solfataricus* P2 attached with a thin layer of ConA-stained material and single cells were visible, which were connected to each other or to the surface by thin filament-like structures (Fig. 3, first row (i)). In contrast to this, PBL2025 formed microcolonies surrounded by ConA-stained extracellular material with cells embedded in it (Fig. 3, second row (i)). PBL2025-LacS and PBL2025-ABCE1 displayed a similar microcolony appearance as PBL2025. The EPS is voluminous and thin connections are not apparent (Fig. 3, third and fourth row). However, EPS

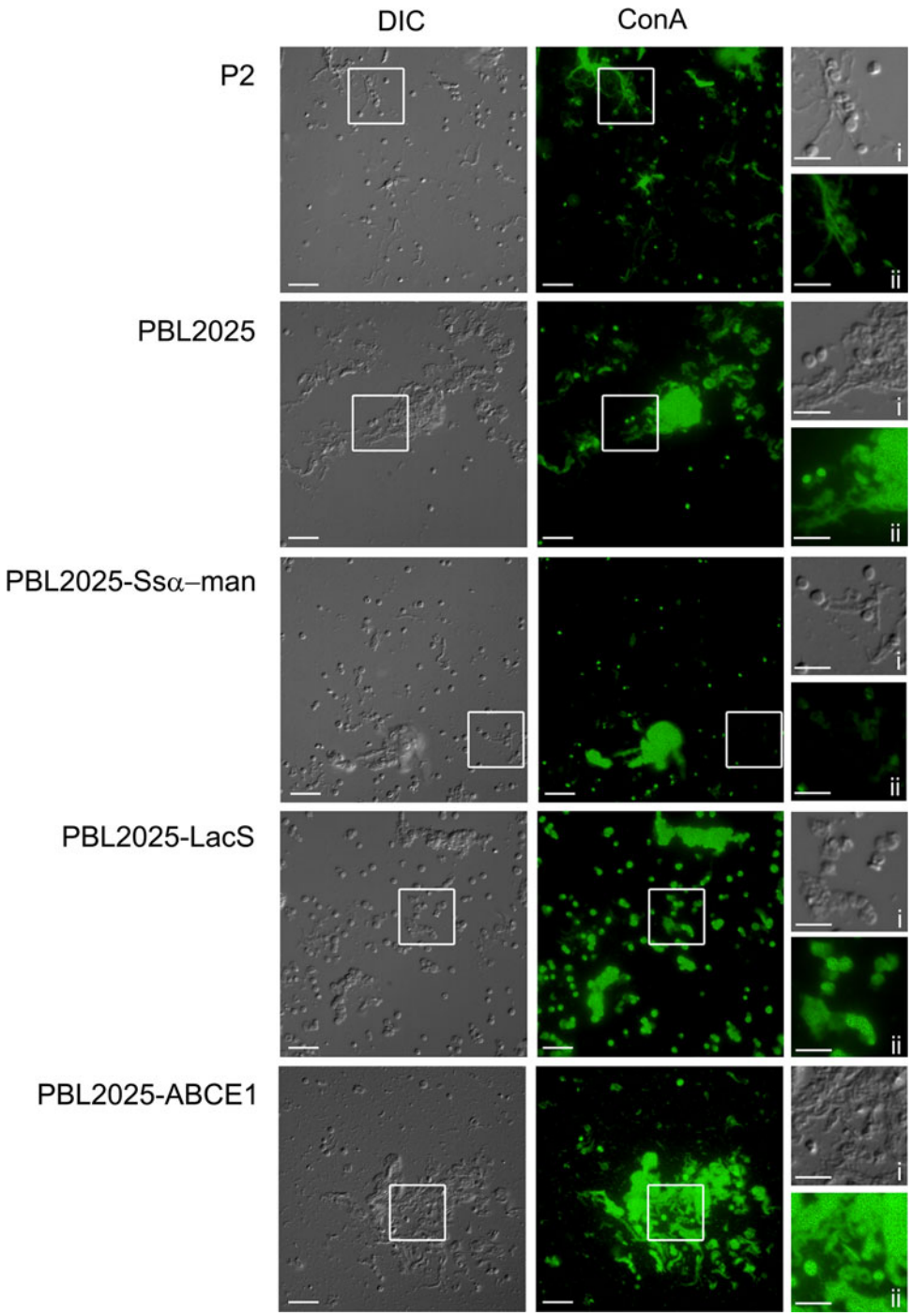

Fig. 3 A 24 h attachment to glass of ConA-stained *S. solfataricus* cells. Surface-attached *S. solfataricus* P2 (depicted as P2), PBL2025, PBL2025, PBL2025-Ssα-man, PBL2025-LacS and PBL2025-ABCE1 were fixed, stained with ConA and analyzed by fluorescence microscopy. In the *first column*, the DIC pictures are illustrated, in the *second column* the ConA stain and in the *third column* the overlay of the DIC and ConA stain (*bars* 10 μm). The *last column* displays a detailed view of the *gray boxes* indicated in the overlay images as DIC (*i*) and ConA (*ii*) pictures with higher magnification (*bars* 5 μm), respectively

of PBL2025-Ssα-man is less voluminous in comparison to PBL2025, but still exhibits a higher amount of EPS than P2 (Fig. 3, third row). Considering the fact that still a number of genes of the 50 kb gene deletion are missing in PBL2025-Ssα-man, it was not unexpected that the phenotype could not completely be reversed by the expression of Ssα-man. However, *S. solfataricus* P2 exhibited a weak ConA signal (Fig. 3, first row (ii)), whereas PBL2025 gave a strong ConA signal (Fig. 3, second row (ii)). The ConA signals for PBL2025-LacS and PBL2025-ABCE1 were comparable to PBL2025 (Fig. 3, third and fourth row) and only in the Ssα-man expressing strain the detected ConA signal was greatly diminished in comparison to PBL2025 (Fig. 3, third row (ii)). Interestingly, the levels of the ConA signal of PBL2025-Ssα-man were comparable to *S. solfataricus* P2 (Fig. 3, third row). Therefore, we concluded that the EPS production of PBL2025-Ssα-man was still higher than that of the *S. solfataricus* P2, but the composition changed, i.e., the amount of mannose/glucose was reduced. This is documented by the ConA signal of the cells, which

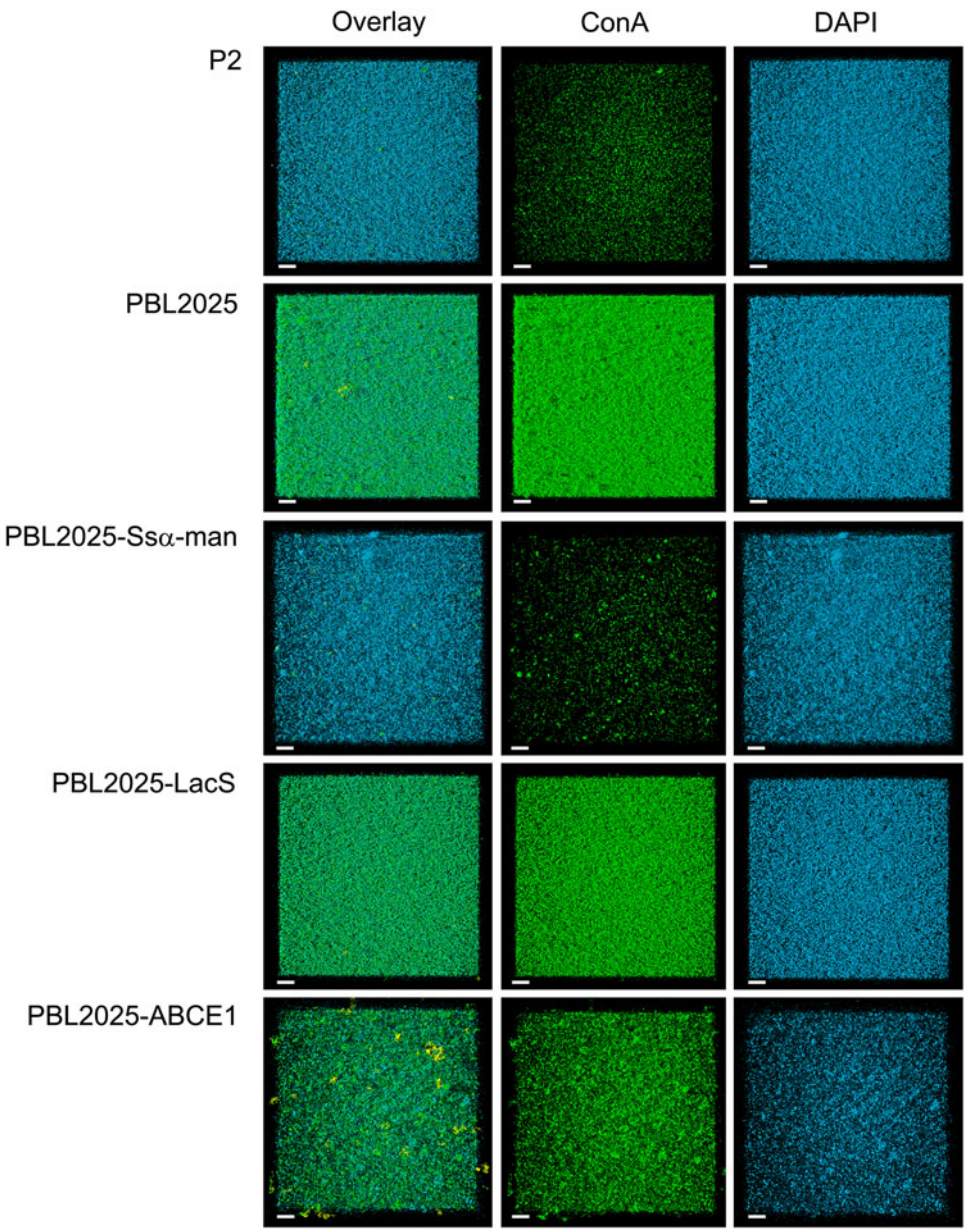

Fig. 4 CLSM-analysis of stained *Sulfolobus* biofilms. The 3-day-old biofilm of *Sulfolobus solfataricus* P2 (depicted as P2), PBL2025, PBL2025-Ssα-man, PBL2025-LacS and PBL2025-ABCE1 were stained with DAPI (*blue*), ConA (*green*) and IB_4 (*yellow*). In the *first column*, the overlay of all three channels is shown; the *second column* shows the ConA stain and the *third column* the DAPI stain. IB_4 signal is only shown in the overlay. *Bars* are 20 μm in length

is reduced in the Ssα-man overexpressing strain with respect to all other strains (Fig. 3, third row (ii)) tested in this study, implying a change in the S-layer glycan or the EPS of this strain.

Biofilm formation of P2, PBL2025 and the recombinant strains

To further explore this phenomenon, we analyzed biofilm formation of all transformed strains. Since the α-mannosidase and *lac*S gene were under control of an arabinose-inducible promoter in the virus vector (Albers et al. 2006), these strains were grown as biofilms in the presence of 0.1% N-Z-amine, 0.2% glucose and 0.2% D-arabinose. The biofilms of *S. solfataricus* P2 and PBL2025 showed the same morphology: both exhibited a confluent appearance and the cell density was comparable (Fig. 4, row 1 and 2, DAPI stain in the last column). Importantly, the infection with the virus vector did not influence or change the phenotype of the PBL2025 biofilm, in contrast to that observed in bacteria (Corbin et al. 2001; Doolittle et al. 1995, 1996; Sutherland et al. 2004). PBL2025 and PBL2025-LacS showed the same phenotype with respect to cell density and lectin staining (Fig. 4, line 2 and 34). In the PBL2025-ABCE1 biofilm the cell density was lower, which possibly indicated an effect of the expression of ABCE1 influencing the cell growth under these conditions (Fig. 4, row 5). In contrast to this, the biofilm of PBL2025-Ssα-man was comparable with the *S. solfataricus* P2 biofilm (Fig. 4, row 3). The ConA signal was strongly reduced and resembled

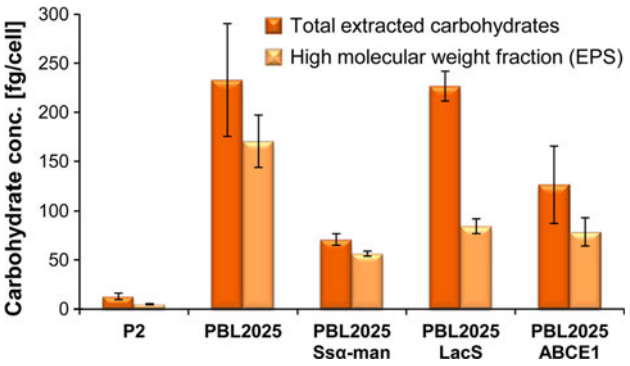

Fig. 5 Carbohydrate concentration in the non-dialyzed and dialyzed cell-free supernatants of biofilms of *S. solfataricus* P2 (depicted as P2), PBL2025, PBL2025-LacS PBL2025-ABCE1 and PBL2025-Ssα-man

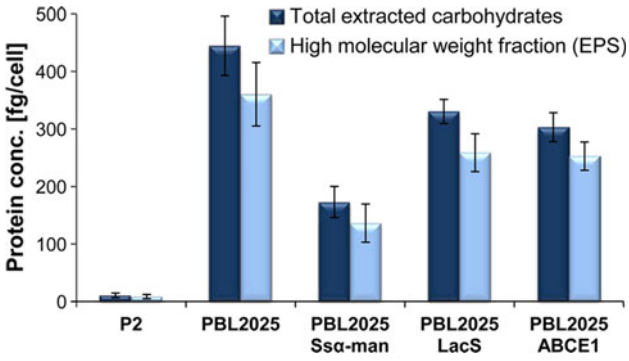

Fig. 6 Protein concentration in the non-dialyzed and dialyzed cell-free supernatants of biofilms of *S. solfataricus* P2 (depicted as P2), PBL2025, PBL2025-LacS PBL2025-ABCE1 and PBL2025-Ssα-man

S. solfataricus P2 levels (Fig. 4, row 3). The ConA signal of the biofilm of PBL2025 and the control strains, PBL2025-LacS and PBL2025-ABCE1 (Fig. 4, row 4 and 5), had a similar intensity, like that of surface-attached cells (Fig. 3). Therefore, all these strains exhibited more EPS or S-layer proteins containing glucose or mannose than *S. solfataricus* P2. Moreover, the complementation of PBL2025 with α-mannosidase led to a phenotype, which was comparable to *S. solfataricus* P2, with respect to the ConA signal.

EPS characterization

To determine differences in the composition and quantity of EPS components during biofilm formation, *S. solfataricus* P2, PBL2025, PBL2025-Ssα-man, PBL2025-LacS and PBL2025-ABCE1 were grown as biofilms on gellan gum-solidified Brock medium containing either 0.1% tryptone and 0.2% glucose or 0.1% N-Z-amine, 0.2% glucose and 0.2% D-arabinose. After EPS extraction using a cation exchange resin (Dowex), the protein and carbohydrate contents of the non-dialyzed cell-free supernatant (i.e., total amount of extracellular carbohydrates and proteins including low molecular weight substances) and the dialyzed cell-free supernatant (EPS) with respect to total cell number were determined (Figs. 5, 6).

For *S. solfataricus* P2, the analyses revealed a rather low total carbohydrate concentration of 12.78 fg/cell (Fig. 5). The vast majority of the measured carbohydrates in *S. solfataricus* P2 was of low molecular weight (<14 kDa) and, thus, was removed by dialysis leading to a concentration of EPS carbohydrates of 4.82 fg/cell. For PBL2025, PBL2025-LacS and PBL2025-ABCE1, a significantly increased carbohydrate production per cell was observed, which contained a significantly higher percentage of high molecular weight compounds. PBL2025 and PBL2025-LacS revealed a 17-fold higher carbohydrate concentration compared to *S. solfataricus* P2 of which 73 and 37% were of high molecular weight, respectively. PBL2025-ABCE1 showed only a slightly higher concentration of total carbohydrates compared to *S. solfataricus* P2. However, the EPS carbohydrate content made up 62% and, therefore, by far exceeded the EPS carbohydrate content in *S. solfataricus* P2. PBL2025-Ssα-man showed a significantly reduced total carbohydrate concentration similar to *S. solfataricus* P2 with 80% being EPS carbohydrates.

Protein quantification revealed a similar trend as observed for carbohydrates (Fig. 6). All strains exhibited protein concentrations of 11–445 fg/cell with 78–83% being EPS proteins. *S. solfataricus* P2 showed the lowest production (11 fg/cell) of EPS proteins followed by PBL2025-Ssα-man (136 fg/cell). The highest concentration of proteins was found in the natural mutant PBL2025. Determination of total proteins of this mutant led to a concentration of 445 fg/cell, with 81% being EPS proteins.

Discussion

Previously, we observed that *S. solfataricus* P2 and PBL2025 exhibit different phenotypes upon adhesion to surfaces (Zolghadr et al. 2010). PBL2025 produced more extracellular material during surface attachment, which contained high levels of sugars including glucose, mannose, galactose and *N*-acetyl-D-glucosamine. In contrast to *S. solfataricus*, P2 PBL2025 lacks 50 genes that are presumably involved in sugar metabolism, degradation and synthesis (Schelert et al. 2004). Therefore, we expressed the two only characterized enzymes of this gene region, LacS (Cubellis et al. 1990) and the Ssα-man (Cobucci-Ponzano et al. 2010), in PBL2025 to monitor their effect on EPS production and surface protein glycosylation during attachment and biofilm formation.

Although biofilm formation of PBL2025 on plastic surfaces (Petri dishes) appeared similar to the one of

S. solfataricus P2 with respect to cell density and biofilm thickness, detection of Glc/Man residues by fluorescently labeled ConA revealed that similar to that in microcolonies on glass slides, PBL2025 produced either more exopolysaccharide containing Glc/Man residues and/or exhibited a significant change in the glycosylation of its cell surface-associated or extracellular proteins (Fig. 1). Strikingly, the expression of the Ssα-man in PBL2025 resulted in a similar phenotype as *S. solfataricus* P2 with respect to EPS production and surface protein glycosylation in surface attachment and biofilm formation assays. In contrast, the expression of LacS as well as ABCE1 did not alter the appearance of the biofilm with respect to the ConA signal. Only for the ABCE1 expressing strain, a decrease in cell density of the biofilm was observed compared to the other strains (Fig. 4, row 5). ABCE1 is a cytoplasmic protein involved in ribosome recycling and its overexpression might have an effect on cells; however, this effect was not observed during growth curves (data not shown) or surface attachment (Fig. 3, row 5). It is important that, although the cell density of the PBL2025-ABCE1 was lower during biofilm formation than in *S. solfataricus* P2, the ConA signal was comparable to the one of PBL2025.

To address if the expression of the Ssα-man in PBL2025 has a major effect on EPS formation, the amount and overall carbohydrate and protein composition of EPS of all strains was analyzed biochemically. Strains P2 and PBL2025 clearly showed an increased production of EPS, which was reflected in the elevated carbohydrate as well as in the protein content of the extracellular material of strain PBL2025. This further confirmed the hypothesis that the 50 genes lacking in PBL2025 compared to *S. solfataricus* P2 might be involved in the modulation of the EPS. The identity of the extracellular carbohydrates and proteins is still to be investigated. Potential components of extracellular material may be exopolysaccharides (Mescher and Strominger 1976), S-layer derived glycosylated proteins, membrane vesicles coated with S-layer proteins (Ellen et al. 2009) as well as flagella and pili (Schopf et al. 2008) released from the biofilm cells.

Although the expression of LacS and ABCE1 had no effect on the ConA binding to biofilms visualized by CLSM, the quantitative EPS analysis showed a decrease in protein and carbohydrate content of the EPS, which was a bit more pronounced in the SSα-man complemented strain. The reduced formation of EPS by the ABCE1 expression strain was rather unexpected; however, as already indicated by the decreased cell density of the biofilm a major effect is observed, which, however, did not influence ConA binding.

Therefore, the expression of Ssα-man in PBL2025 seemed to have a significant effect, which resulted in a phenotype of biofilm formation and EPS production resembling that of *S. solfataricus* P2. As ConA binds preferably to mannose or glucose residues and the Ssα-man hydrolyzes high-mannose oligosaccharides as well as de-mannosylates *N*-glycosylated proteins (Rnase B) (Cobucci-Ponzano et al. 2010), it is most likely that the amount of mannose as a component of glycoproteins changed depending on the absence or presence of Ssα-man. This raised the question whether the Ssα-man expression may affect the glycan tree of glycosylated proteins.

According to the current understanding, the archaeal N-glycosylation pathway resembles the eukaryal one, in which ER located α-mannosidases play a crucial role in the trimming of the glycan tree or might also be involved in the degradation and catabolism of glycoproteins (Herscovics 1999; Nakajima et al. 2003). A main function of the intracellularly localized Ssα-man in *N*-glycan processing was proposed previously from in vitro studies (Brock et al. 1972), as the glycan tree was assembled at the cytoplasmic side of the membrane and an overexpression of the cytoplasmic Ssα-man might lead to the de-mannosylation of the glycan tree before transfer of the mature glycoprotein to the extracellular side of the membrane. This would result in a reduced mannosylation of cell surface-associated proteins and—as observed in our experiments—a reduction of the ConA binding to biofilm cells in CLSM analysis. Therefore, these studies offer first evidence for a possible in vivo function of the cytoplasmic Ssα-man of *S. solfataricus* in trimming of the glycan tree.

Taken together, our study has yielded the following observations: (1) the lack of 50 genes in PBL2025 leads to a change of the sugar composition of the EPS/surface proteins in biofilms; (2) the complementation of PBL2025 with cytoplasmic α-mannosidase (SSO3306) partially restored the phenotype of *S. solfataricus* P2 during surface attachment and biofilm formation and supports an in vivo function of the enzyme in trimming of the glucan tree. Moreover, an EPS isolation method developed for efficient EPS extraction of bacterial pure-culture and mixed-population biofilms (Nielsen and Jahn 1999) was successfully applied to isolate EPS from *Sulfolobus* biofilms, which will enable further studies on the composition, secretion and function of EPS synthesis during *Sulfolobus* biofilm formation.

References

Abu-Qarn M, Yurist-Doutsch S, Giordano A, Trauner A, Morris HR, Hitchen P, Medalia O, Dell A, Eichler J (2007) *Haloferax volcanii* AglB and AglD are involved in N-glycosylation of the S-layer glycoprotein and proper assembly of the surface layer. J Mol Biol 374:1224–1236

Albers SV, Meyer BH (2011) The archaeal cell envelope. Nat Rev Microbiol 9:414–426

Albers SV, Elferink MG, Charlebois RL, Sensen CW, Driessen AJ, Konings WN (1999) Glucose transport in the extremely

thermoacidophilic *Sulfolobus solfataricus* involves a high-affinity membrane-integrated binding protein. J Bacteriol 181:4285–4291

Albers SV, Jonuscheit M, Dinkelaker S, Urich T, Kletzin A, Tampe R, Driessen AJ, Schleper C (2006) Production of recombinant and tagged proteins in the hyperthermophilic archaeon *Sulfolobus solfataricus*. Appl Environ Microbiol 72:102–111

Antón J, Meseguer I, Rodríguez-Valera F (1988) Production of an extracellular polysaccharide by *Haloferax mediterranei*. Appl Environ Microbiol 54:2381–2386

Baker-Austin C, Potrykus J, Wexler M, Bond PL, Dopson M (2010) Biofilm development in the extremely acidophilic archaeon '*Ferroplasma acidarmanus*' Fer1. Extremophiles 14:485–491

Barthelme D, Scheele U, Dinkelaker S, Janoschka A, Macmillan F, Albers SV, Driessen AJ, Stagni MS, Bill E, Meyer-Klaucke W, Schunemann V, Tampe R (2007) Structural organization of essential iron-sulfur clusters in the evolutionarily highly conserved ATP-binding cassette protein ABCE1. J Biol Chem 282:14598–14607

Barthelme D, Dinkelaker S, Albers SV, Londei P, Ermler U, Tampe R (2011) Ribosome recycling depends on a mechanistic link between the FeS cluster domain and a conformational switch of the twin-ATPase ABCE1. Proc Natl Acad Sci USA 108:3228–3233

Bartolucci S, Rossi M, Cannio R (2003) Characterization and functional complementation of a nonlethal deletion in the chromosome of a beta-glycosidase mutant of *Sulfolobus solfataricus*. J Bacteriol 185:3948–3957

Brock TD, Brock KM, Belly RT, Weiss RL (1972) *Sulfolobus*: a new genus of sulfur-oxidizing bacteria living at low pH and high temperature. Arch Mikrobiol 84:54–68

Cobucci-Ponzano B, Conte F, Strazzulli A, Capasso C, Fiume I, Pocsfalvi G, Rossi M, Moracci M (2010) The molecular characterization of a novel GH38 alpha-mannosidase from the crenarchaeon *Sulfolobus solfataricus* revealed its ability in de-mannosylating glycoproteins. Biochimie 92:1895–1907

Corbin BD, McLean RJ, Aron GM (2001) Bacteriophage T4 multiplication in a glucose-limited *Escherichia coli* biofilm. Can J Microbiol 47:680–684

Cubellis MV, Rozzo C, Montecucchi P, Rossi M (1990) Isolation and sequencing of a new á-galactosidase-encoding archaebacterial gene. Gene 94:89–94

Doolittle MM, Cooney JJ, Caldwell DE (1995) Lytic infection of *Escherichia coli* biofilms by bacteriophage T4. Can J Microbiol 41:12–18

Doolittle MM, Cooney JJ, Caldwell DE (1996) Tracing the interaction of bacteriophage with bacterial biofilms using fluorescent and chromogenic probes. J Ind Microbiol 16:331–341

Dubois M, Gilles KA, Hamilton JK, Rebers PA, Smith F (1956) Colorimetric method for determination of sugars and related substances. Anal Chem 28:350–356

Ellen AF, Albers SV, Huibers W, Pitcher A, Hobel CFV, Schwarz H, Folea M, Schouten S, Boekema EJ, Poolman B, Driessen AJM (2009) Proteomic analysis of secreted membrane vesicles of archaeal Sulfolobus species reveals the presence of endosome sorting complex components. Extremophiles 13:67–79

Flemming HC, Wingender J (2010) The biofilm matrix. Nat Rev Microbiol 8:623–633

Herscovics A (1999) Importance of glycosidases in mammalian glycoprotein biosynthesis. Biochim Biophys Acta 1473:96–107

Jonuscheit M, Martusewitsch E, Stedman KM, Schleper C (2003) A reporter gene system for the hyperthermophilic archaeon *Sulfolobus solfataricus* based on a selectable and integrative shuttle vector. Mol Microbiol 48:1241–1252

Kelly J, Logan SM, Jarrell KF, VanDyke DJ, Vinogradov E (2009) A novel *N*-linked flagellar glycan from *Methanococcus maripaludis*. Carbohydr Res 344:648–653

Koerdt A, Gödeke J, Berger J, Thormann KM, Albers SV (2010) Crenarchael biofilm formation under extreme conditions. PlosOne 5:e14104

Maruyama Y, Nakajima T, Ichishima E (1994) A 1, 2-alpha-D-mannosidase from a *Bacillus* sp.: purification, characterization, and mode of action. Carbohydr Res 251:89–98

Mescher MF, Strominger JL (1976) Purification and characterization of a prokaryotic glucoprotein from the cell envelope of *Halobacterium salinarium*. J Biol Chem 251:2005–2014

Moracci M, Ciaramella M, Rossi M (2001) Beta-glycosidase from *Sulfolobus solfataricus*. Methods Enzymol 330:201–215

Nakajima M, Imamura H, Shoun H, Wakagi T (2003) Unique metal dependency of cytosolic alpha-mannosidase from *Thermotoga maritima*, a hyperthermophilic bacterium. Arch Biochem Biophys 415:87–93

Nicolaus B, Manca MC, Ramano I, Lama L (1993) Production of an exopolysaccharide from two thermophilic archaea belonging to the genus *Sulfolobus*. FEMS Microbiol Lett 109:203–206

Nielsen PH, Jahn A (eds) (1999) Extraction of EPS. Springer, Berlin

Paramonov NA, Parolis LA, Parolis H, Boán IF, Antón J, Rodríguez-Valera F (1998) The structure of the exocellular polysaccharide produced by the *Archaeon Haloferax gibbonsii* (ATCC 33959). Carbohydr Res 309:89–94

Petersen GL (1977) A simplification of the protein assay of Lowry which is more generally applicable. Anal Chem 83:346–353

Peyfoon E, Meyer B, Hitchen PG, Panico M, Morris HR, Haslam SM, Albers SV, Dell A (2010) The S-layer glycoprotein of the crenarchaeote *Sulfolobus acidocaldarius* is glycosylated at multiple sites with chitobiose-linked *N*-glycans. Archaea. doi: 10.1155/2010/754101

Rinker KD, Kelly RM (1996) Growth Physiology of the Hyperthermophilic Archaeon *Thermococcus litoralis*: development of a sulfur-free defined medium, characterization of an exopolysaccharide, and evidence of biofilm formation. Appl Environ Microbiol 62:4478–4485

Rinker KD, Kelly RM (2000) Effect of carbon and nitrogen sources on growth dynamics and exopolysaccharide production for the hyperthermophilic archaeon *Thermococcus litoralis* and bacterium *Thermotoga maritima*. Biotechnol Bioeng 69:537–547

Sampaio MM, Chevance F, Dippel R, Eppler T, Schlegel A, Boos W, Lu YJ, Rock CO (2004) Phosphotransferase-mediated transport of the osmolyte 2-*O*-alpha-mannosyl-D-glycerate in *Escherichia coli* occurs by the product of the mngA (hrsA) gene and is regulated by the mngR (farR) gene product acting as repressor. J Biol Chem 279:5537–5548

Schelert J, Dixit V, Hoang V, Simbahan J, Drozda M, Blum P (2004) Occurrence and characterization of mercury resistance in the hyperthermophilic archaeon *Sulfolobus solfataricus* by use of gene disruption. J Bacteriol 186:427–437

Schopf Simone, Gerhard Wanner, Reinhard Rachel, Wirth (2008) An archaeal bi-species biofilm formed by *Pyrococcus furiosus* and *Methanopyrus kandleri*. Arch Microbiol 190:371–377

Sumper M, Berg E, Mengele R, Strobel I (1990) Primary structure and glycosylation of the S-layer protein of *Haloferax volcanii*. J Bacteriol 172:7111–7118

Sutherland IW, Hughes KA, Skillman LC, Tait K (2004) The interaction of phage and biofilms. FEMS Microbiol Lett 232:1–6

Voisin S, Houliston RS, Kelly J, Brisson JR, Watson D, Bardy SL, Jarrell KF, Logan SM (2005) Identification and characterization of the unique *N*-linked glycan common to the flagellins and S-layer glycoprotein of *Methanococcus voltae*. J Biol Chem 280:16586–16593

Zahringer U, Moll H, Hettmann T, Knirel YA, Schafer G (2000) Cytochrome b558/566 from the archaeon *Sulfolobus acidocaldarius* has a unique Asn-linked highly branched hexasaccharide chain containing 6-sulfoquinovose. Eur J Biochem 267:4144–4149

Zolghadr B, Weber S, Szabo Z, Driessen AJ, Albers SV (2007) Identification of a system required for the functional surface localization of sugar binding proteins with class III signal peptides in *Sulfolobus solfataricus*. Mol Microbiol 64:795–806

Zolghadr B, Klingl A, Koerdt A, Driessen AJ, Rachel R, Albers SV (2010) Appendage-mediated surface adherence of *Sulfolobus solfataricus*. J Bacteriol 192:104–110